Frontiers of Information Technology & Electronic Engineering
www.jzus.zju.edu.cn; engineering.cae.cn; www.springerlink.com
ISSN 2095-9184 (print); ISSN 2095-9230 (online)
E-mail: jzus@zju.edu.cn

Modeling yarn-level geometry from a single micro-image*

Hong-yu WU†‡, Xiao-wu CHEN†, Chen-xu ZHANG†, Bin ZHOU†, Qin-ping ZHAO

State Key Laboratory of Virtual Reality Technology and Systems, School of Computer Science and Engineering, Beihang University, Beijing 100191, China

†E-mail: whyvrlab@buaa.edu.cn; chen@buaa.edu.cn; zhangchenxu528@buaa.edu.cn; zhoubin@buaa.edu.cn

Received Nov. 4, 2018; Revision accepted Mar. 11, 2019; Crosschecked Aug. 23, 2019

Abstract: Different types of cloth show distinctive appearances owing to their unique yarn-level geometrical details. Despite its importance in applications such as cloth rendering and simulation, capturing yarn-level geometry is nontrivial and requires special hardware, e.g., computed tomography scanners, for conventional methods. In this paper, we propose a novel method that can produce the yarn-level geometry of real cloth using a single micro-image, captured by a consumer digital camera with a macro lens. Given a single input image, our method estimates the large-scale yarn geometry by image shading, and the fine-scale fiber details can be recovered via the proposed fiber tracing and generation algorithms. Experimental results indicate that our method can capture the detailed yarn-level geometry of a wide range of cloth and reproduce plausible cloth appearances.

Key words: Single micro-images; Yarn geometry; Cloth appearance
https://doi.org/10.1631/FITEE.1800693 **CLC number:** TP391.9

1 Introduction

Capturing and rendering realistic cloth appearance is important for applications such as cloth animation (Wang et al., 2011), human performance capture and rendering (Li et al., 2013; Liu et al., 2013; Xu et al., 2014; Zhu et al., 2017), and virtual try on. However, this task is still challenging, because real-world cloths have complex and varying geometries at the yarn level, which makes their surface reflectance functions spatially varying and anisotropic. Therefore, it is crucial to deliver an effective method for capturing yarn geometry.

To accurately obtain a real-world yarn geometry, Zhao et al. (2012, 2014, 2016) proposed a method for modeling yarns from three-dimensional (3D) volumetric data captured by a micro-computed tomography (CT) scanner. Their methods can trace every individual 3D fiber and reproduce a volumetric cloth model according to the user-specified fabric designs. These methods can recover high-resolution volumetric yarns and fibers, and the output is of high resolution and physically correct. However, considering the expensive hardware required and the time cost, the need for a micro-CT scanner greatly restricts the applicability of the methods, especially for common users in their daily life.

The volumetric cloth model needs massive amounts of random access memory (RAM) or disk storage. Schröder et al. (2015) proposed a procedural yarn model that uses several intuitive parameters to generate complex yarns. Furthermore, they proposed an image-based method for automatic analysis of weaving patterns. Although their method works well for woven fabrics, it may fail for other types such as knitted fabrics.

In this study, we propose a novel method for modeling yarn-level geometry on the surface from a single image (Fig. 1). Compared with existing

‡ Corresponding author
* Project supported by the National Natural Science Foundation of China (Nos. 61532003 and 61902014) and the National Key Research and Development Plan, China (No. 2018YFC0831003)
ORCID: Hong-yu WU, http://orcid.org/0000-0002-8127-3347

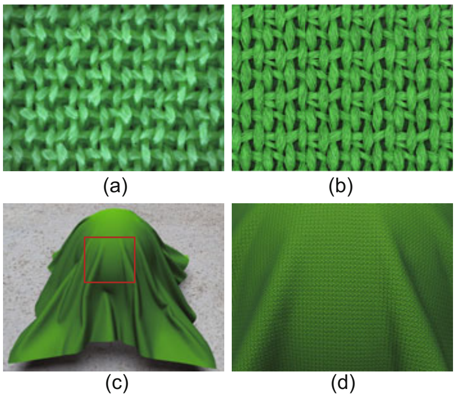

Fig. 1 Given a single micro-image of a cloth sample (a), our method can recover the yarn-level geometry with fiber details (b). This enables realistic rendering of the cloth mesh (c) and a close-up view of the rendering result (d)

methods, the proposed technique can handle different types of cloths. More importantly, it is designed to be widely available in daily life at a low cost. Internet applications, virtual dressing, and virtual reality can also benefit from our method. The only input is a single image captured by a consumer digital camera. To this end, we build a novel yarn database containing the micro-images from 60 different kinds of cloth. Guided by the database, the yarn layout can be recovered. To further model the fibers of yarn, we propose techniques that trace individual fibers in the image and generate dense fiber geometry details. Experimental results show that our method can recover plausible yarn-level geometry.

Different from yarn-level cloth design and modeling (Yuksel et al., 2012; Leaf et al., 2018), the inner yarn structure is ignored in our study, because the cloth appearances depend mostly on the yarn-level geometry of the cloth surface.

The contributions of this study are summarized as follows: (1) a novel framework to capture the yarn-level geometry from a single image; (2) techniques for automatic yarn layout and shape recovery, fiber tracing, and generation. Overall, the proposed method shows a good potential for being used in real applications because it is effective, inexpensive, and easy to use.

2 Related work

In this section, we review the existing works that are related to cloth micro-geometry capture and the fiber scattering function.

2.1 Cloth micro-geometry

The small-scale structure is a key factor of fabric appearance. Capturing the small-scale structure is important for realistic fabric rendering. The data from CT scanning can provide extremely detailed volumetric information about fibers. The fibers are traced in the discrete CT data, and the cloth micro structure is recovered from the traced fibers. Based on fiber tracing, the volumetric fibers of woven cloth are built from CT data, and the optical parameters of the volumetric fibers are estimated from the images (Zhao et al., 2014). Given the volumetric fabric samples, a new volumetric cloth model has been created according to the user-specified fabric designs (Zhao et al., 2012).

The procedural models are used to generate the small-scale 3D structure. The interlaced/intertwisted displacement subdivision surface is used to represent the fabric micro-structure of woven fabric (Zhang et al., 2013). Schröder et al. (2015) presented a procedural yarn model based on the state-of-the-art results from textile research. This model statistically describes the yarn structure using several parameters. Based on the yarn model, an automatic parsing approach from a single image was proposed to estimate the parameters of the model and the weave pattern. Zhao et al. (2016) proposed an end-to-end pipeline for automatically fitting the CT measurements using Schröder et al. (2015)'s procedural yarn model. The flyaway fiber model was improved for creating high-quality cloth rendering results with fiber-level details. Our study also uses Schröder et al. (2015)'s procedural yarn model to generate the fiber-level cloth geometry model.

An elastic material coated with specially designed powder is used to contact the object surface. The powder replaces the uncontrolled surface material, so that the photometric stereo algorithm can be used to recover the micro-geometry precisely (Johnson et al., 2011). However, the elastic material cannot fully contact the gap between curved yarns and the contact pressure may lead to yarn shape deformation.

The multi-view or multi-light technology has been used to capture the bidirectional reflectance distribution function (BRDF) and geometry of a surface (Zhou et al., 2013; Nam et al., 2016). However, the gap between curved yarns is relatively deep, which may lead to occlusion of light and obvious inter-reflection. Moreover, calibrating the camera and lights before the capture is tedious.

2.2 Fiber scattering function

The scattering characteristic of single fibers has been explored for a long time. Marschner et al. (2003) illuminated an individual hair with a narrow beam of various directions and measured the scattered light at various positions. An analytical scattering function that models the surface reflection, refractive transmission, and internal reflection was used to fit the measurements. Similarly, the scattering measurements of a single yarn were acquired with a fully automatic, four-axis image-based gonioreflectometer in Sadeghi et al. (2013). The yarn scattering function uses two Gaussian lobes to model the surface reflectance and volume scattering. The cloth BRDF model is the weighted sum of all the yarn scattering functions. Irawan and Marschner (2012) proposed a procedural yarn scattering model with a small set of parameters which describe the fiber scattering characteristics, the geometry of the yarns, and the pattern of the weave. They simplified the light transport inside the yarn, so that the complex light scattering can be described by some simple equations derived from the yarn geometry. The cloth micro-geometry models can produce realistic rendering results with extreme fiber details. A new cloth appearance matching framework to determine the optical parameters of the geometry model was proposed in Khungurn et al. (2015). The optical parameters of the micro-geometry model were optimized to match the appearance photographs taken under many different lighting conditions.

3 Overview

We estimate the yarn geometry parameters through three steps (Fig. 2). We first extract the unit patch and yarn layout. The yarn layout accounts for the number, two-dimensional (2D) size, and locations of yarns. Then we recover the geometry of every yarn using image shading (Section 4). Finally, 2D fibers are traced in the images and the 3D fibers are fitted to them. The recovered yarn shapes with fiber details are used to produce the final output (Section 6).

We first describe the yarn geometry model of yarns used in this study. The surface of knit or weave cloth has a periodic texture. The global cloth appearance can be represented by the spatial duplication of a unit path. The yarn layout describes the size, location, and rotation of the yarn segments in the unit path, and the geometry of every yarn is modeled by two parts, its shape and fibers.

To model and detect the yarn layout from an image, we introduce a 3×3 grid (Sudoku) for yarn layout representation (Fig. 3a). Yarn modeling or detection is performed on the center grid, and the yarn layout is copied to the other eight squares in the grid. If a yarn layout is valid, the area of the overlapping region between the yarns or blank region in the Sudoku grid is small. Fig. 3 shows two yarn layouts. The left is a valid layout and the right is an invalid one.

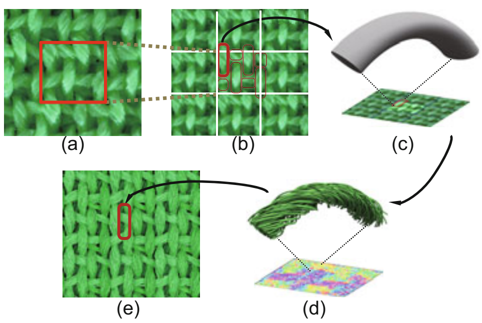

Fig. 2 Pipeline of yarn geometry capture. The input is a micro-image of a cloth sample (a) captured under a circular light. First, we extract the unit patch and yarn layout (b). The yarn shape (c) parameters are then estimated by image shading. Next, the yarn twist angle is estimated based on the traced fiber (d). Finally, we obtain the yarn-level geometry (e) from the estimated yarn parameters

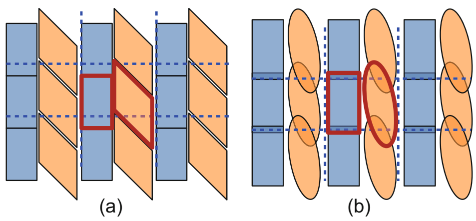

Fig. 3 A 3×3 grid representation of yarn layout. The layout in (a) has a small overlapping region; it can be treated as a valid layout. The layout in (b) has an obvious overlapping region; it is an invalid layout

The yarn shape is designed based on the state-of-the-art yarn model proposed by Irawan and Marschner (2012). Fig. 4 illustrates the yarn shape, which is a curved cylinder with width w and

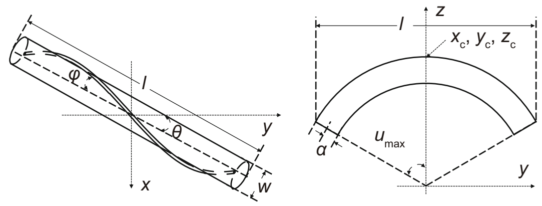

Fig. 4 Parameterization of the outer shape and location of yarn. Some parameters are not shown in this figure: the yarn curvature κ can be found in Irawan and Marschner (2012); fiber count m and migration $R_{\min}$ can be found in Schröder et al. (2015)

projection length l. The cross-section of the cylinder is an ellipse with long axis $w/2$ and short axis α. The curvature of the cylinder is controlled by $u_{\max}$ and κ. The relationship between the parameters was described in Irawan and Marschner (2012). The parameters (x_c, y_c, z_c) indicate the location of the top of the curved cylinder. The yarn rotation angle around the z axis is denoted by θ.

The fiber model is a simplified version of the procedural model in Schröder et al. (2015), because a single micro-image is not sufficient for estimating the full range of parameters. We found that a single-ply yarn is sufficient for modeling the appearance of the yarn surface, even if the yarn has multiple plies. Flyaway fibers are not considered in this study. The original version of the procedural yarn model used nine parameters to control the fibers of a ply. In our study, we use two parameters: fiber twisting φ and fiber count m. The other parameters are constant.

4 Yarn layout extraction

We use the periodic pattern detection technology from Asha et al. (2012) to extract the unit patch (Fig. 3b). Owing to cloth distortion, there are obvious discontinuities when putting the unit patch on a 3×3 grid. This makes the yarn detection and fiber tracing step difficult. We employ the image quilting technology to reduce the blockiness when putting the unit patch together (Efros and Freeman, 2001). The yarn layout can be extracted by detecting the yarns inside or across the center grid based on the 3×3 representation. We use a deformable-part model (DPM) (Felzenszwalb et al., 2010) to detect the yarn bounding box. The DPM is trained using the discriminative learning algorithm (latent support vector machine (SVM)), which needs only yarn bounding boxes from the yarn database. The DPM algorithm can detect only the vertical yarns, but the yarns of knitted cloth are not vertical or horizontal. To make DPM compatible with those yarns, we rotate the 3×3 grid by 60 angles uniformly sampled between 0° and 180°. Then the detected bounding boxes are rotated back to the original position. After the above steps, we can obtain several bounding boxes on the center grid and manually delete the incorrect bounding boxes. The periodic pattern and yarn detection methods may fail in some cases, so we manually adjust the detection results. The yarn length l, width w, rotation θ, and the position on the image (x_c, y_c) of every yarn can be computed directly from the detected bounding boxes.

5 Yarn shape estimation

Under uniform environmental light, a surface point will be shaded darker if it lies deeper. This simple phenomenon is known as "dark is deep," and inspired by this, we propose to estimate the yarn shape according to the pixel intensity values (an orthogonal projection assumption for the micro-image capture is made in this study). In particular, we assume that the relationship between surface depth and corresponding pixel intensity can be modeled by a linear function. The scaling factor converting pixel intensity values to depth values is determined by cloth thickness, which can be either estimated or assigned by the user. In addition, if the captured image contains yarns with different colors, they should be separated and re-grouped according to their colors in advance, and this can be done using the image matting technique (Chen et al., 2013b) with required user strokes. Note that in such cases, the scaling factor should be calculated separately for different yarn areas.

Owing to the complex fiber structure, the raw depth estimated from the image is also noisy. Accordingly, we remove the high-frequency component from the yarn shape using the weighted least squares (WLS) edge-preserving filter (Farbman et al., 2008) and retain the global shading information produced by illumination (Chen et al., 2013a). Figs. 5a and 5b show the image capture process and captured image, respectively. Fig. 5c shows the yarn depth estimated from a single image and we can obtain the yarn shape parameters by fitting the yarn shape model to the depth image.

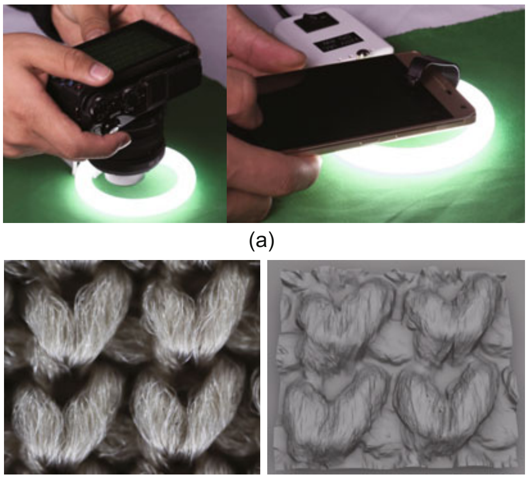

Fig. 5 Yarn depth from image shading: (a) image capture process; (b) captured image; (c) yarn surface depth

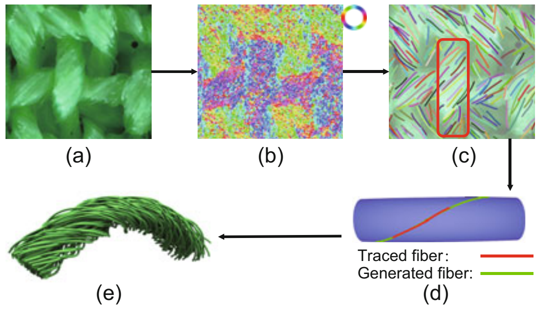

Fig. 6 Illustration of fiber tracing. We first calculate the fiber orientation of every pixel from the unit patch (a) and discretize the orientation map into sticks (b). Next, we trace the fibers stick by stick (the color lines in (c)). (d) is fiber fitting. We fit the fiber parametric model to the traced fiber to obtain the twisting angle and obtain the generation of fiber (e). References to color refer to the online version of this figure

6 Fiber tracing and generation

Inspired by Chai et al. (2012, 2015), we trace the fibers of every yarn to estimate the twist angle. We first detect the fiber orientation of every pixel on the center patch of the 3×3 grid using the same orientation filters (Chai et al., 2012). Different from hair images, the micro-image of fabric is noisy owing to fiber specular reflection, translucence, and impurities, which introduce noise into the orientation map. Thus, we discretize the orientation map into rectangular sticks with rotation angle $\hat{\theta}$ (Fig. 6). The blending angle difference between the covered orientations and $\hat{\theta}$ is minimized:

$$\arg\min \sum_{p \in \Omega} B(\tilde{\theta}(p), \hat{\theta}), \tag{1}$$

where Ω is the region covered by the stick, p the image coordinate, $\tilde{\theta}$ the detected orientation map, and $B(\cdot,\cdot)$ the blending angle $(0, \pi/2)$ between two orientations.

The orientation map discretization is implemented by iteratively filling the grid with sticks. During each iteration, a stick is placed at the point that has the maximum distance to the filled region. In our case, the maximum distance can be computed by distance transform. The stick orientation is computed using Eq. (1). The iteration stops when there is insufficient space to contain a stick. Note that the discretization is performed on the center patch of the 3×3 grid. When a stick is put on the center patch, eight of the same sticks are simultaneously put on the other eight patches.

Similar to the approach in Chai et al. (2012, 2015), we trace a stick sequence belonging to a single fiber by moving from one stick to another from a seed stick, and the seed stick is selected randomly. We start tracing from a seed pixel in both directions from its center to its two ends. At the current stick, the untraced sticks are selected as candidate sticks from the radius (four times the stick length in our experiment) around the end of the stick sequence. The stick that has the minimum blending angle is selected from the candidate sticks, and the selected stick is set to be traced. The tracing stops when the traced fiber reaches out of the yarn region. When the tracing step finishes, we connect the stick sequence and obtain a traced fiber.

We have revealed the yarn outer shape through the previous steps, so the yarn twisting can be estimated according to the traced fibers. The yarn twisting φ of a fiber can be estimated by fitting the procedural model to the traced fiber. Based on the matched shape in Section 4, the fiber count m of every yarn is set to $m = 0.3\alpha w/r^2$, where r is the fiber radius and the default value is 4.5 μm in our study. From our observations, we find that the width of a fiber takes up 8–10 pixels in the micro-image.

7 Results

Our prototype system was implemented in Matlab on a PC with a quad-core CPU (Intel i7–4790) and 16 GB memory. For a unit patch with about 1000×1000 pixels, the total time to recover the yarn-level geometry from a single micro-image was about 15 min. The only user interaction required was manual adjustment of the yarn and unit patch detection, which took about an additional 3–5 min for a trained user to finish.

In our experiment, we generated 200–400 fibers for each yarn and the fibers were stored as a polyline. The cloth was constructed by repeating the yarns along the x- and y-axis by the size of the unit patch. We rendered the fibers using the physics-based renderer (Jakob, 2010). We can recover the plausible yarn-level geometry of a variety of cloths not limited to woven cloth. The advantage of our method is that we need only one micro-image. Fig. 7 shows the yarn-level geometry of nine different kinds of cloth, including six knit cloths and three weave cloths. The yarns of knit cloth are no longer aligned vertically, which makes them difficult to capture; another advantage of our method is that we can capture the complex yarn geometry of knit cloth. The two advantages of our method reveal its potential for future consumer applications owing to its low-cost nature.

The cloth appearance is affected mainly by the location of specular reflection, specular and diffuse albedo, and yarn glossiness. To simulate the appearance of cloth/garment mesh, we consider the state-of-the-art yarn texture model proposed by Irawan and Marschner (2012). The specular reflection location is determined by the yarn layout and yarn shape. The yarn specular and diffuse albedo and glossiness are determined by the yarn optical properties, including k_s, k_d, α, β, and δ. The micro-image cannot represent optical properties of the yarn: a cloth appearance photo is necessary for estimating the yarn optical parameters. For the purpose of daily use, we use the same lightweight configuration (a mobile phone camera and built-in flash) as that in Aittala et al. (2015) to capture a cloth image for appearance matching. Fig. 8 shows the rendering results at different scales using the estimated optical parameter: the cloth appearance model can generate the yarn details on the cloth surface, and rendering results have similar visual effect to the captured photo.

The Sudoku representation allows the user to design new cloth. Users can add or delete a yarn at the center grid and, at the same time, our system copies the yarn layout to the other eight grids, which guarantees that the users can immediately preview the yarn layout. The user can adjust the yarn location, rotation, or size to make the yarn layout repeatable. Fig. 9 shows two user designs, which took 10 min of manual interaction. After that, our system can generate the yarn geometry and cloth appearance model.

8 Conclusions and future work

In this paper, we have proposed a novel method that can capture the yarn-level geometry of cloth from a single micro-image. We used a Sudoku representation for yarn layout. The yarn shape was estimated by image shading and the fiber details were recovered by fiber tracing. Experimental results indicated that our method can capture the plausible detailed yarn-level geometry. Our techniques also showed a good potential for various applications because it is very easy to use for non-experts and the required hardware is widely available and inexpensive.

8.1 Limitations

The yarn layout detection of our method is heavily reliant on the periodic features of the cloth image, and therefore the micro-geometry of certain cloth types such as velvet cannot be recovered by our method (Fig. 10a). Our method often fails when the cloth is seriously distorted or has a high density of flyaway fibers on the surface (Figs. 10b and 10c). When the cloth is made of high-transparency yarns, the yarn cannot be detected easily. We used image shading to estimate the yarn shape, so our method cannot recover the yarn shapes accurately when a cloth is made of yarns of different colors.

8.2 Future work

A major limitation of our approach is the manual correction of yarn layout detection results, which is difficult for amateurs. A data-driven strategy based on deep learning such as those in Chai et al. (2016) and Zhang et al. (2017) can be explored to achieve automatic yarn geometry capture. Capturing the micro-geometry and appearance of cloth with yarns of different colors is still a difficult problem, and requires further investigation. A cloth shader for real-time rendering that can enhance the yarn details of cloth also needs to be explored in future work. We do not deal with the knotting of the yarns in this study. We just simply place

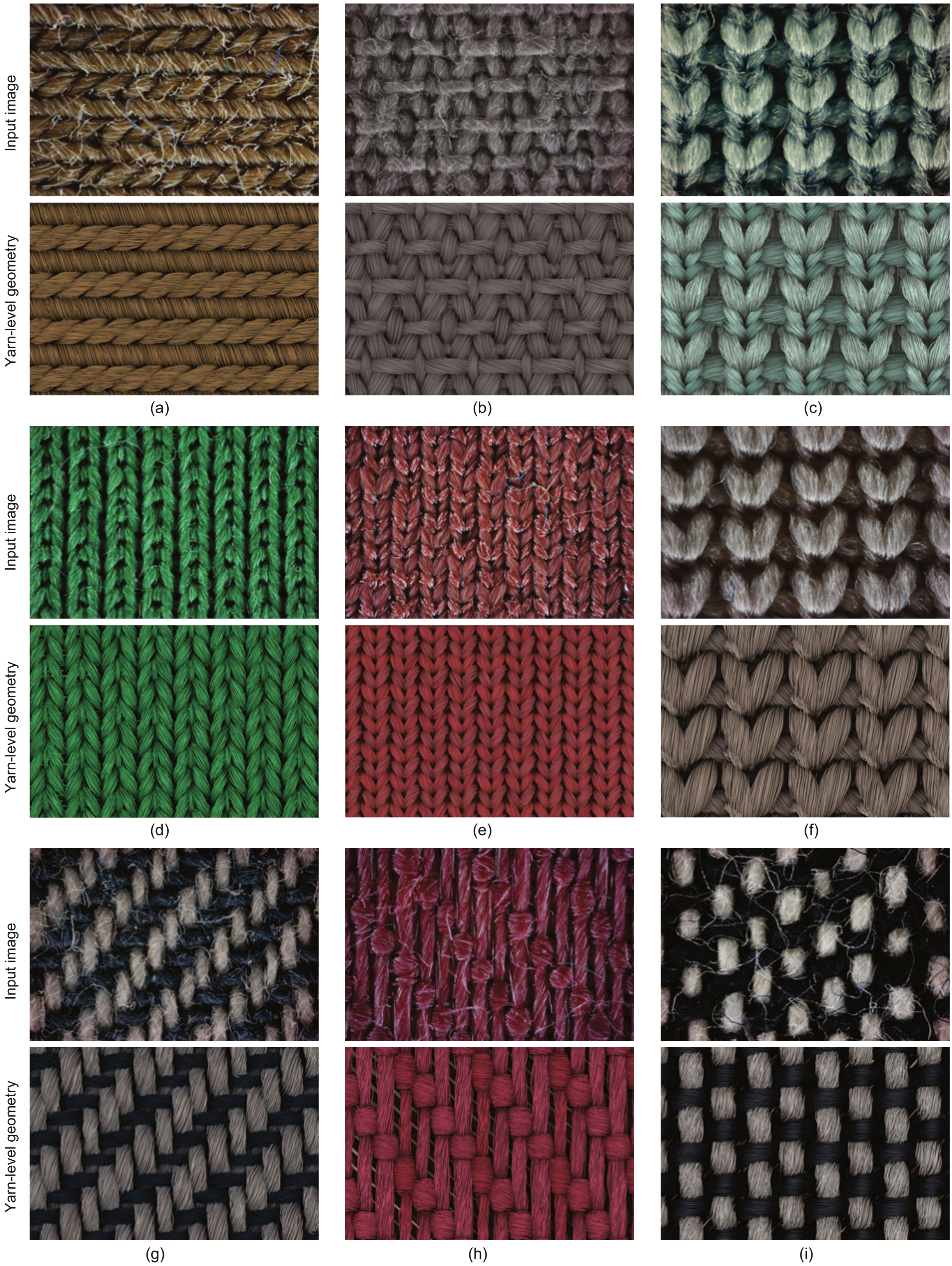

Fig. 7 Experimental results for yarn-level geometry recovery. We show nine different kinds of cloth in this figure. The first six ((a)–(f)) are knit cloth and the last three ((g)–(i)) are weave cloth

Fig. 8 Three appearance rendering results using estimated parameters. The top row shows the three appearance images. Rows 2–4 show the recovered yarn geometry (a), cloth mesh rendering results (b), and close-up view (c)

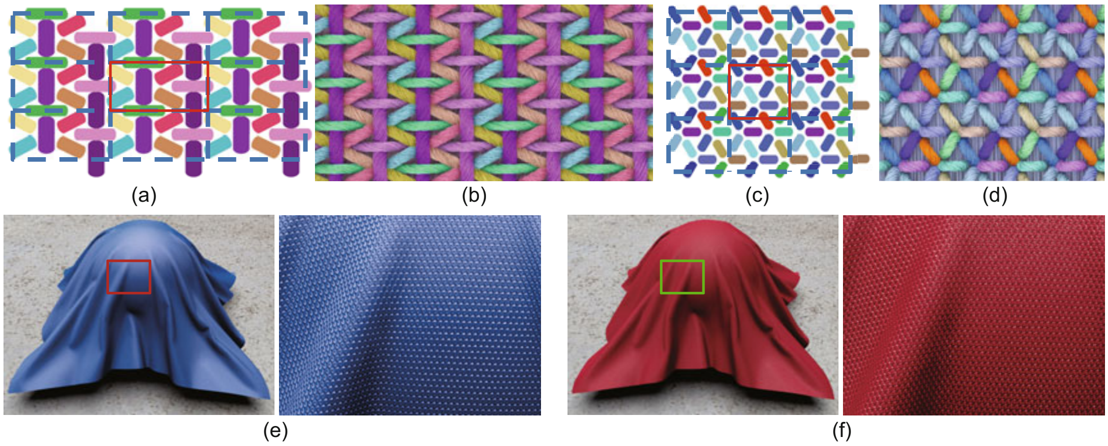

Fig. 9 User-designed weave patterns: (a) and (c) are designed weave patterns, (b) and (d) are yarn geometries generated according to the user design, and (e) and (f) are cloth appearance rendering results of (a) and (c) respectively

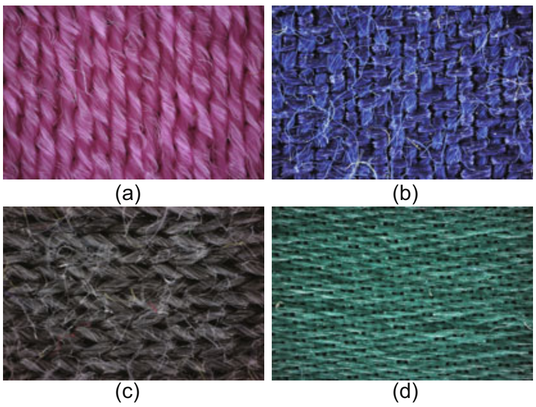

Fig. 10 Four cases where our method failed: (a) cloth with no periodic features on the surface; (b) seriously distorted cloth; (c) cloth with heavy density of flyaway fibers on the surface; (d) cloth made of high-transparency yarns

the detected yarn segments together without really connecting and knotting them together. In future work, the entire weave structure can be inferred from a single micro-image, which can benefit the yarn-level simulation of woven cloth (Cirio et al., 2014).

Compliance with ethics guidelines

Hong-yu WU, Xiao-wu CHEN, Chen-xu ZHANG, Bin ZHOU, and Qin-ping ZHAO declare that they have no conflict of interest.

References

Aittala M, Weyrich T, Lehtinen J, 2015. Two-shot SVBRDF capture for stationary materials. *ACM Trans Graph*, 34(4), Article 110. https://doi.org/10.1145/2766967

Asha V, Nagabhushan P, Bhajantri NU, 2012. Automatic extraction of texture-periodicity using superposition of distance matching functions and their forward differences. *Patt Recogn Lett*, 33(5):629-640. https://doi.org/10.1016/j.patrec.2011.11.027

Chai ML, Wang LD, Weng YL, et al., 2012. Single-view hair modeling for portrait manipulation. *ACM Trans Graph*, 31(4), Article 116. https://doi.org/10.1145/2185520.2185612

Chai ML, Luo LJ, Sunkavalli K, et al., 2015. High-quality hair modeling from a single portrait photo. *ACM Trans Graph*, 34(6), Article 204. https://doi.org/10.1145/2816795.2818112

Chai ML, Shao TJ, Wu HZ, et al., 2016. AutoHair: fully automatic hair modeling from a single image. *ACM Trans Graph*, 35(4), Article 116. https://doi.org/10.1145/2897824.2925961

Chen XW, Wu HY, Jin X, et al., 2013a. Face illumination manipulation using a single reference image by adaptive layer decomposition. *IEEE Trans Image Process*, 22(11):4249-4259. https://doi.org/10.1109/TIP.2013.2271548

Chen XW, Zou DQ, Zhou SZ, et al., 2013b. Image matting with local and nonlocal smooth priors. Proc IEEE Conf on Computer Vision and Pattern Recognition, p.1902-1907. https://doi.org/10.1109/CVPR.2013.248

Cirio G, Lopez-Moreno J, Miraut D, et al., 2014. Yarn-level simulation of woven cloth. *ACM Trans Graph*, 33(6), Article 207. https://doi.org/10.1145/2661229.2661279

Efros AA, Freeman WT, 2001. Image quilting for texture synthesis and transfer. Proc 28th Annual Conf on Computer Graphics and Interactive Techniques, p.341-346. https://doi.org/10.1145/383259.383296

Farbman Z, Fattal R, Lischinski D, et al., 2008. Edge-preserving decompositions for multi-scale tone and detail manipulation. *ACM Trans Graph*, 27(3), Article 67. https://doi.org/10.1145/1360612.1360666

Felzenszwalb PF, Girshick RB, McAllester D, et al., 2010. Object detection with discriminatively trained part-based models. *IEEE Trans Patt Anal Mach Intell*, 32(9):1627-1645. https://doi.org/10.1109/TPAMI.2009.167

Irawan P, Marschner S, 2012. Specular reflection from woven cloth. *ACM Trans Graph*, 31(1), Article 11. https://doi.org/10.1145/2077341.2077352

Jakob W, 2010. Mitsuba Physically Based Renderer. http://www.mitsuba-renderer.org.

Johnson MK, Cole F, Raj A, et al., 2011. Microgeometry capture using an elastomeric sensor. *ACM Trans Graph*, 30(4), Article 46. https://doi.org/10.1145/2010324.1964941

Khungurn P, Schroeder D, Zhao S, et al., 2015. Matching real fabrics with micro-appearance models. *ACM Trans Graph*, 35(1), Article 1. https://doi.org/10.1145/2818648

Leaf J, Wu RD, Schweickart E, et al., 2018. Interactive design of periodic yarn-level cloth patterns. *ACM Trans Graph*, 37(6), Article 202. https://doi.org/10.1145/3272127.3275105

Li GN, Wu CL, Stoll C, et al., 2013. Capturing relightable human performances under general uncontrolled illumination. *Comput Graph Forum*, 32(2pt3):275-284. https://doi.org/10.1111/cgf.12047

Liu LB, Yin KK, Wang B, et al., 2013. Simulation and control of skeleton-driven soft body characters. *ACM Trans Graph*, 32(6), Article 215. https://doi.org/10.1145/2508363.2508427

Marschner SR, Jensen HW, Cammarano M, et al., 2003. Light scattering from human hair fibers. *ACM Trans Graph*, 22(3):780-791. https://doi.org/10.1145/882262.882345

Nam G, Lee JH, Wu HZ, et al., 2016. Simultaneous acquisition of microscale reflectance and normals. *ACM Trans Graph*, 35(6), Article 185. https://doi.org/10.1145/2980179.2980220

Sadeghi I, Bisker O, de Deken J, et al., 2013. A practical microcylinder appearance model for cloth rendering. *ACM Trans Graph*, 32(2), Article 14. https://doi.org/10.1145/2451236.2451240

Schröder K, Zinke A, Klein R, 2015. Image-based reverse engineering and visual prototyping of woven cloth. *IEEE Trans Vis Comput Graph*, 21(2):188-200. https://doi.org/10.1109/TVCG.2014.2339831

Wang HM, O'Brien JF, Ramamoorthi R, 2011. Data-driven elastic models for cloth: modeling and measurement. *ACM Trans Graph*, 30(4), Article 71. https://doi.org/10.1145/2010324.1964966

Xu WW, Umentani N, Chao QW, et al., 2014. Sensitivity-optimized rigging for example-based real-time clothing synthesis. *ACM Trans Graph*, 33(4), Article 107. https://doi.org/10.1145/2601097.2601136

Yuksel C, Kaldor JM, James DL, et al., 2012. Stitch meshes for modeling knitted clothing with yarn-level detail. *ACM Trans Graph*, 31(4), Article 37. https://doi.org/10.1145/2185520.2185533

Zhang JH, Baciu G, Zheng DJ, et al., 2013. IDSS: a novel representation for woven fabrics. *IEEE Trans Vis Comput Graph*, 19(3):420-432. https://doi.org/10.1109/TVCG.2012.66

Zhang M, Chai ML, Wu HZ, et al., 2017. A data-driven approach to four-view image-based hair modeling. *ACM Trans Graph*, 36(4), Article 156. https://doi.org/10.1145/3072959.3073627

Zhao S, Jakob W, Marschner S, et al., 2012. Structure-aware synthesis for predictive woven fabric appearance. *ACM Trans Graph*, 31(4), Article 75. https://doi.org/10.1145/2185520.2185571

Zhao S, Jakob W, Marschner S, et al., 2014. Building volumetric appearance models of fabric using micro CT imaging. *ACM Commun*, 57(11):98-105. https://doi.org/10.1145/2670517

Zhao S, Luan FJ, Bala K, 2016. Fitting procedural yarn models for realistic cloth rendering. *ACM Trans Graph*, 35(4), Article 51. https://doi.org/10.1145/2897824.2925932

Zhou ZL, Wu Z, Tan P, 2013. Multi-view photometric stereo with spatially varying isotropic materials. Proc IEEE Conf on Computer Vision and Pattern Recognition, p.1482-1489. https://doi.org/10.1109/CVPR.2013.195

Zhu H, Liu YB, Fan JT, et al., 2017. Video-based outdoor human reconstruction. *IEEE Trans Circ Syst Video Technol*, 27(4):760-770. https://doi.org/10.1109/TCSVT.2016.2596118